



ELSEVIER

Available online at www.sciencedirect.com

SCIENCE @ DIRECT®

Earth and Planetary Science Letters 239 (2005) 140–161

EPSL

www.elsevier.com/locate/epsl

Addressing solar modulation and long-term uncertainties in scaling secondary cosmic rays for in situ cosmogenic nuclide applications

Nathaniel A. Lifton^{a,*}, John W. Bieber^b, John M. Clem^b, Marc L. Duldig^c,
Paul Evenson^b, John E. Humble^d, Roger Pyle^b

^a*Geosciences Department, University of Arizona, Tucson, AZ 85721, USA*

^b*Bartol Research Institute, University of Delaware, Newark, DE 19716, USA*

^c*Australian Antarctic Division, Kingston, Tasmania, 7050, Australia*

^d*School of Mathematics and Physics, University of Tasmania, Private Bag 37, Hobart, Tasmania, 7001, Australia*

Received 16 December 2004; accepted 1 July 2005

Available online 24 August 2005

Editor: K. Farley

Abstract

Solar modulation affects the secondary cosmic rays responsible for in situ cosmogenic nuclide (CN) production the most at the high geomagnetic latitudes to which CN production rates are traditionally referenced. While this has long been recognized (e.g., D. Lal, B. Peters, Cosmic ray produced radioactivity on the Earth, in: K. Sitte (Ed.), *Handbuch Der Physik XLVI/2*, Springer-Verlag, Berlin, 1967, pp. 551–612 and D. Lal, Theoretically expected variations in the terrestrial cosmic ray production rates of isotopes, in: G.C. Castagnoli (Ed.), *Proceedings of the Enrico Fermi International School of Physics 95*, Italian Physical Society, Varenna, 1988, pp. 216–233), these variations can lead to potentially significant scaling model uncertainties that have not been addressed in detail. These uncertainties include the long-term (millennial-scale) average solar modulation level to which secondary cosmic rays should be referenced, and short-term fluctuations in cosmic ray intensity measurements used to derive published secondary cosmic ray scaling models. We have developed new scaling models for spallation nucleons, slow-muon capture and fast-muon interactions that specifically address these uncertainties. Our spallation nucleon scaling model, which includes data from portions of 5 solar cycles, explicitly incorporates a measure of solar modulation (S), and our fast- and slow-muon scaling models (based on more limited data) account for solar modulation effects through increased uncertainties. These models improve on previously published models by better sampling the observed variability in measured cosmic ray intensities as a function of geomagnetic latitude, altitude, and solar activity. Furthermore, placing the spallation nucleon data in a consistent time-space framework allows for a more realistic assessment of uncertainties in our model than in earlier ones.

We demonstrate here that our models reasonably account for the effects of solar modulation on measured secondary cosmic ray intensities, within the uncertainties of our combined source datasets. We also estimate solar modulation variations over the last 11.4 ka from a recent physics-based sunspot number reconstruction derived from tree-ring ^{14}C data. This approximation suggests that spallation nucleon scaling factors in our model for sea level and high geomagnetic latitudes can differ by up to

* Corresponding author. Tel.: +1 520 626 3251; fax +1 520 621 2672.

E-mail address: lifton@geo.arizona.edu (N.A. Lifton).

~10%, depending on the time step over which the model sunspot numbers are averaged. The potential magnitude of this difference supports our contention that incorporating long-term solar modulation into secondary cosmic ray scaling is important. Although millennial-scale solar modulation clearly requires further study, we believe it is reasonable at present to use our S value record for scaling spallogenic nucleons during the last 11.4 ka, and the weighted mean S value for that period of 0.950 for longer exposure times. By accounting for solar modulation effects on the global variations in nucleon and muon fluxes, these models thus provide a useful framework on which to base CN production rate scaling functions.

© 2005 Elsevier B.V. All rights reserved.

Keywords: solar activity; scaling models; production rates; spallogenic nucleons; muons; cutoff rigidity

1. Introduction

A cornerstone of in situ cosmogenic nuclide (CN) applications is the ability to scale production rates from the few sites where they are well established to sites under study. This is necessary because the intensity of secondary cosmic rays responsible for in situ CN production varies with both altitude and position within the geomagnetic field. However, models used for this purpose often do not explicitly account for uncertainties arising from the natural variability inherent in the assumptions and data used in their development. Sources of these uncertainties include solar cycle variations and other variability of the primary cosmic ray flux considered against limited periods of record, and discrepancies between parameterizations of modern and time-integrated geomagnetic field effects on cosmic rays. We have developed scaling models for secondary cosmic ray nucleons and muons, and a model for time-integrated geomagnetic effects on cosmic rays, that specifically address these uncertainties with an eye toward application to CN production over millennial time scales.

1.1. Controls on cosmic ray intensity

The primary cosmic rays incident on the Earth's atmosphere consist of 90% protons and 8% helium nuclei (also called α particles) with the remainder being heavier nuclei and electrons [1]. The nuclear particles interact with atmospheric nuclei to produce a cascade of secondary particles, which are ultimately responsible for in situ CN production. At a given location on the Earth's surface, there are two main controls on the flux of these secondary particles (both of which vary temporally and spatially, e.g., [2,3]): the

geomagnetic field and the mass of atmosphere traversed by the particles. Secondary influences on cosmic ray intensities include solar variability (e.g., [4]) and spectral variations in the primary flux (e.g., [5]). CN production rate scaling models based on modern measurements of cosmic ray intensities need to be able to account for the variation in each of these factors, and to generalize cosmic ray measurements made over limited time frames to representative values for millennial time scales.

1.1.1. Quantifying geomagnetic and atmospheric influences

Because the primary particles are charged, the geomagnetic field exerts a strong influence on their trajectories (and therefore, on the geographic distribution of their progeny). This influence can be quantified through the concept of cutoff rigidity. Cutoff rigidity is defined as the minimum rigidity (momentum per unit charge, R , usually measured in GV) that an incident primary cosmic ray particle may possess and still be able to interact with the atmosphere at a given location [6,7]. Rigidity has been denoted by both R and P in the cosmic ray literature. We follow the convention of [6] and represent it using R , to avoid confusion with the typical use of P for CN production rates. Cutoff rigidity has an inverse relationship with geomagnetic latitude (λ)—it is low near the poles where essentially all incoming cosmic rays are admitted, and higher near the equator.

Effective vertical cutoff rigidity (R_C) expands on this definition by accounting for the effects of the zone of alternating allowed and forbidden cosmic ray trajectories near the Earth known as the penumbral region, which results from the interaction of complex, looping cosmic ray trajectories with the solid Earth [6,8]. R_C has typically been calculated numeri-

cally by tracing the path of vertically incident anti-protons outward from 20 km above the Earth's surface in a static, high-order spherical harmonic approximation to the geomagnetic field (e.g., [8]). Accounting for obliquely incident particles generally has only a second-order effect on the relationship between R_C and measured intensities, but has helped explain small deviations in observations [9]. Over the last 2 decades, however, it has become apparent that dynamic solar wind effects on the geometry of the Earth's magnetosphere also influence measured cosmic ray intensities, and must be accounted for in detailed studies (e.g., [10–12]). R_C has proven to be quite robust as a means of parameterizing cosmic ray intensity measurements (e.g., [13,14]). Essentially all studies of atmospheric variations in cosmic ray intensity published since the early 1960s recognize this, and use R_C as their ordering parameter ([7], and references therein).

The other principal control on cosmic ray intensity at a given location is the mass of atmosphere (represented as atmospheric depth (X) in g cm^{-2}) traversed by the incident cosmic rays at that location. Between atmospheric depths of approximately 200 g cm^{-2} ($\sim 12 \text{ km}$ altitude) and 1033 g cm^{-2} (sea level), energy-integrated cosmic ray intensities (I) exhibit an approximately exponential absorption with increasing depth. This can be characterized by an attenuation length (A , in g cm^{-2}),

$$A = \frac{X_1 - X_2}{\ln(I_2) - \ln(I_1)} \quad (1)$$

where I_1 and I_2 are the intensities measured at atmospheric depths X_1 and X_2 , respectively. One should note that A varies with R_C by ~ 10 to 15% (e.g., [15]), implying a corresponding variation in the nucleon energy spectrum. Attenuation length has also been referred to as absorption length, absorption mean free path, and attenuation mean free path in the cosmic ray and CN literature (e.g., [16–18]). Attenuation length has the advantage of being easy to use for scaling cosmic ray intensities between different altitudes or pressures. However, we view A as less than ideal for CN scaling models appropriate for millennial time scales, since the observed variability (scatter) in the data is lost or reduced in the calculation (i.e., the entire I vs. X profile is

reduced to one value). Moreover, while this scatter can be quantified with an uncertainty in A , that uncertainty is magnified exponentially with increasing differences in X when propagated in scaling models, potentially leading to inaccurate estimates of model uncertainties.

1.1.2. Quantifying solar influences

Solar activity fluctuates in a cyclic manner over a variety of time scales. The well-known solar cycles with periods of 11 (sunspot, or Schwabe cycle) and 22 yr (magnetic, or Hale cycle) are thought to be modulated by cycles with periods of 88 (Gleissberg cycle), 208 (Suess cycle), and possibly 2300 yr (Hallstatt cycle) [4,19]. These variations cause turbulence in the solar wind, whose ionized particles carry solar-magnetic fields outward from the sun. Variations and irregularities in these magnetic fields interact with the inward flow of galactic cosmic rays, strongly modulating low-energy cosmic rays (rigidities $< 1 \text{ GV}$), while higher energy particles are less affected [5,20,21]. As such, solar cycle variability in cosmic ray intensity (and A) is greatest in areas of low R_C (high λ) values, since a large proportion of low-energy primaries are admitted there (Fig. 1). Conversely, at higher R_C (low λ) values, solar modulation effects are minimal, since low-energy particles are already excluded from those regions [22,23]. Thus, the data used in developing *in situ* CN production rate scaling models are most variable precisely at the R_C values to which the production rates are typically referenced.

Cosmic ray intensities are lowest during times of increased solar activity (solar maximum), and vice-versa. The magnitude of this variation decreases with increasing R_C and X since higher rigidity particles are required to generate deeper penetrating cascades. At low R_C values, the nucleon intensity variation from solar maximum to solar minimum since the 1950s has generally ranged from approximately 15 to 25% between 680 g cm^{-2} (3.4 km altitude) and 307 g cm^{-2} (9.1 km altitude), but only between about 10 to 20% at sea level (1033 g cm^{-2}) (Fig. 1) ([22], University of New Hampshire Neutron Monitor Datasets: http://ulysses.sr.unh.edu/NeutronMonitor/neutron_mon.html, World Data Center for Cosmic Rays (WDCCR): http://www.env.sci.ibaraki.ac.jp/database/html/WDCR/data_e.html). At

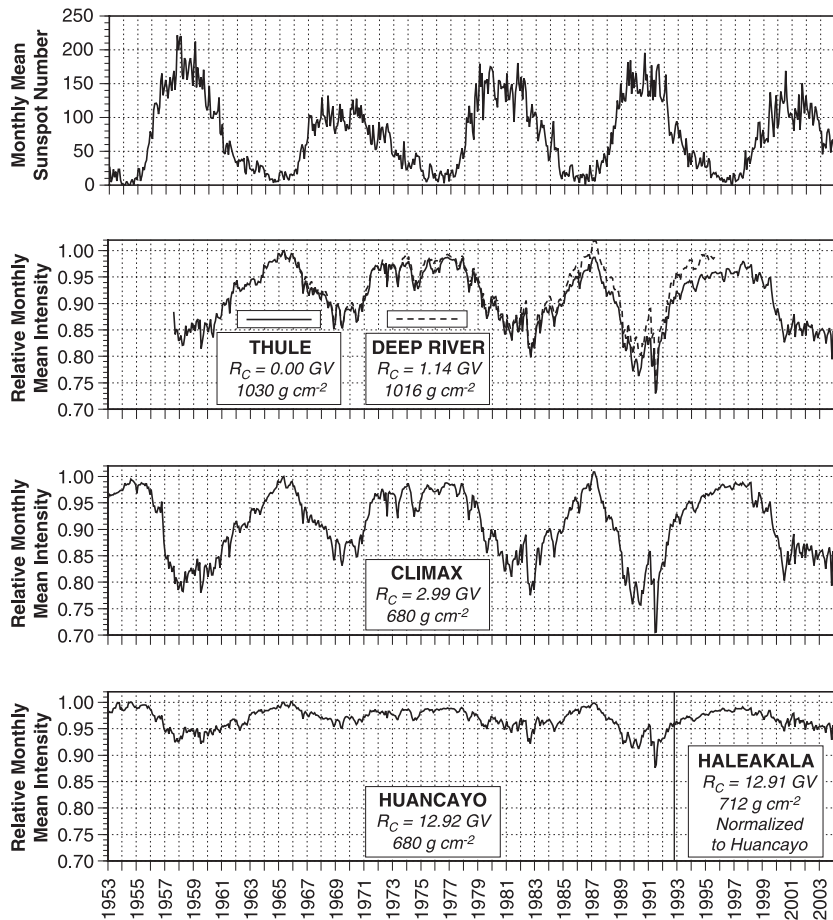


Fig. 1. Monthly mean sunspot numbers and relative intensities for 4 pertinent permanent neutron monitors from 1953 to 2004. Each neutron monitor record has been normalized to its monthly mean intensity during May 1965. Note that the relative maxima and minima for Thule and Climax are generally very similar even though they are at significantly different altitudes (near sea level and 3.4 km, respectively) and slightly different R_C values. The solid vertical line in late 1992 on the Huancayo/Haleakala record marks the point when Huancayo was shut down and Haleakala took over.

high R_C values over the same time period, solar modulation has affected nucleon intensities by $\leq \sim 7\%$ between 680 and 307 $g\ cm^{-2}$, with smaller effects at sea level [13,20,22,24,25]. For comparison, the average variation of A for nucleons typically ranged between about 2 and 4% between 1957 and 1969 at low R_C values, and was negligible at high R_C locations [26]—implying solar modulation effects on the atmospheric nucleon energy spectrum.

Muons are produced in the atmosphere by primary particles of higher median energy than those responsible for secondary nucleons and, therefore, are less affected by solar modulation. Sea level integral muon

intensities ($>0.3\ GeV/c$ momentum) varied by approximately 6 and 4% between the 1965 solar minimum and 1969 solar maximum at R_C values of 2 and 14 GV, respectively [27]. Furthermore, sea level slow-muon intensities ($\sim 0.3\ GeV/c$) varied by approximately 8 and 4%, respectively, over that period at the same cutoff values [27].

While these cyclic variations in solar activity should generally average out over time, they are superimposed on lower frequency fluctuations. For published CN scaling models, it is typically assumed that the solar modulation averages to an intermediate value (e.g., [28,29]), although Desilets and Zreda [15]

suggest solar minimum conditions may approximate the long-term average. Several periods during which solar activity was considerably reduced relative to modern solar minima have been identified during the Holocene (e.g., the Maunder, Spörer, Wolf, Oort, and Dalton Minima), as have periods of enhanced solar activity relative to modern solar maxima (e.g., the Solar Grand Maximum) [4,30,31]. Reedy et al. [5] and Reedy and Marti [32] suggest that solar activity averaged over the last 10 Ma (evidenced by numerous CN records of solar cosmic rays in meteorites and lunar samples) is broadly similar to modern observations, but may have varied by factors of up to ~ 3 to 5. Reedy et al. [5] also suggest that the galactic cosmic ray flux has remained approximately constant over at least the last 100 ka, but with potential fluctuations of up to 30 to 40% or more. The key point here is that the level to which solar cycle variations average is uncertain, with potentially significant implications for CN production rate scaling.

2. Incorporating variability into secondary cosmic ray scaling

Current CN production rate scaling models use measured cosmic ray A values to relate curves describing the latitudinal variation of the energy-integrated secondary cosmic ray intensity (or flux) at given altitudes [3,15,28,29,33,34]. This approach also entails assumptions about how A varies with altitude and latitude. The resulting functions describing the relative variation of cosmic ray intensity are then normalized to a datum such as measured absolute nuclear disintegration rates [29,33] or nucleon intensity at sea level and the geomagnetic pole [15,28,33,34]. As discussed in Section 1.1.1, the use of A in these models leads to propagated uncertainties which grow exponentially with increasing differences in X , potentially leading to unrealistic uncertainty estimates. Furthermore, since each of these scaling models utilizes only a small portion of the available cosmic ray intensity data, we argue that they do not adequately sample the natural variability in Earth's cosmic ray environment. These sampling problems are a potential issue whenever one relates short instrumental records to long-term averaging processes.

Measured atmospheric cosmic ray intensities reflect spatial and temporal variability in the geomagnetic field, solar modulation of the primary cosmic ray flux, and fluctuations in the galactic cosmic ray energy spectrum. Scaling models based on measured intensities should be able to account for this variability. We have attempted to address this long-term uncertainty in a new spallogenic nucleon scaling model by combining global neutron monitor survey data from portions of five solar cycles. We have also developed new models for scaling fast- and slow-muon intensities (i.e., muogenic production mechanisms), as well as a model addressing uncertainties in time-integrated R_C values. However, we do not address low-energy (<10 MeV) nucleon scaling, which may be important for nuclides such as ^{36}Cl and ^{41}Ca [15], nor any potential long-term variability in the galactic cosmic ray energy spectrum.

We fit the scaling models directly to available nucleon and muon intensity data covering a wide range of latitudes and altitudes, without first deriving an intermediate measure such as A . This allows the model uncertainties to better reflect uncertainties in the data, and avoids the issue of exponential growth in propagated scaling uncertainties with increasing differences in X .

Each scaling model incorporates as much natural and measurement variability as is readily available over the short period of record, to better estimate variability in the cosmic ray environment over millennial time scales. Fits were not weighted because the relative measurement uncertainties generally were quite small compared to the variability in the data. Each model parameterizes cosmic ray intensity in terms of R_C and X . All datasets used in this study except one included barometric pressure data (directly convertible to X). The one study that did not include barometric pressures [22] was parameterized by pressure altitude (i.e., the aircraft followed surfaces of constant pressure)—these were converted to X values using the U.S. Standard Atmosphere [35]. While the U.S. Standard Atmosphere is generally only appropriate for mid-latitude locations, latitudinal variation in atmospheric structure is accounted for by the aircraft's altimeter (which is calibrated to that Standard Atmosphere). For simplicity, we used geometric rather than geopotential altitudes (which account for the decrease in gravitational force with increasing altitude) as input for the atmospheric depth calculations,

since differences are negligible at the altitudes considered here.

The spallogenic nucleon model is also parameterized in terms of a relative solar activity coefficient S , derived below. Limited temporal coverage in the muon data, however, prevented us from effectively incorporating a measure similar to S into the fast- and slow-muon models. As a result, the muon models presented here are static, representing intermediate to minimum solar modulation conditions. We have attempted to account for solar modulation effects in the muon models by increasing the uncertainties by amounts based on calculated sea level modulation values [27]. We describe the muogenic scaling models first because we use them to correct the neutron monitor count rates for muogenic contributions [15,36,37] (Appendix A.1 in the Supplementary data). Uncertainties in the scaling model equations have been propagated using the Law of Combination of Errors (including covariance terms) ([38], and Appendix A.1, Table A1-1 in the Supplementary data). Propagated uncertainties for all other equations neglect covariances.

2.1. Muogenic scaling models

We developed scaling models for fast- (or integral, $I_{\mu f}$) and slow-muon ($I_{\mu s}$) intensities based on the muon monitor surveys of Carmichael et al. [39,40]. Compared to the numerous latitude surveys conducted for neutron monitors, only Carmichael et al. [39,40] provide reliable muon monitor data covering a wide range of altitudes and latitudes ($687 < X < 1033$ g cm⁻², $0.8 < R_C < 13.3$ GV). Muon monitors yield flux-weighted integral intensities for momenta $> \sim 0.3$ to 0.4 GeV c⁻¹. We supplemented these data with airborne muon monitor data digitized from Kent and Pomerantz [24] ($X = 680$ g cm⁻², $1.3 < R_C < 14.1$ GV). Data from each survey were normalized as described in Appendix A.1 in the Supplementary data. The normalized integral muon intensity data ($n = 87$) were then fit (with a squared correlation coefficient $R^2 = 0.995$) using an equation of the form

$$\ln(I_{\mu f,s}) = a_1 + a_2 X + a_3 X^2 + a_4 X R_C + a_5 R_C + a_6 R_C^2 \quad (2)$$

(Fig. 2A, Table A1-1 and Appendix A.1, Table A1-1A in the Supplementary data). In terms of $I_{\mu f}$ (not

$\ln(I_{\mu f})$), the fully propagated model uncertainty (from uncertainties in parameter estimates and variables) ranges from about 0.4 to 2.5% (1σ) between sea level and 6 km altitude. The mean residual for the fit is approximately 0.2% (again in terms of $I_{\mu f}$), while the standard deviation of the residuals is $< 2\%$ (1σ). To estimate the total uncertainty in this model, including that from solar variability, we added in quadrature the 1σ propagated model uncertainty, the 1σ of the percentage residuals, and an assumed additional 5% solar variability (1σ ; the midpoint of the range observed by [27]) in the integral muon flux. The resulting 1σ value ranges from approximately 5 to 6% between sea level and 6 km altitude.

We then used this fast-muon model as a foundation for the slow-muon model by scaling the normalized integral intensities back to sea level. This was done for three reasons. First, the sea level latitude variation of slow muons is thought to be similar to that of high-energy muons [27,41]. Second, the relatively large number of muon monitor measurements enabled better definition of the shape of the latitude variation. Finally, including the scatter in the data allowed a better estimate of measurement variability. These scaled sea level data were then renormalized to be consistent with slow-muon flux measurements at high R_C values [41] (Appendix A.1 in the Supplementary data). We augmented this dataset with slow-muon vertical differential flux data from several studies at various atmospheric depths and R_C values ($232 < X < 1033$ g cm⁻², $0.7 < R_C < 16.3$ GV), and at various solar modulation levels [41–50]. Although Sands [51] also presented slow-muon differential flux data, we did not use them because they represented omnidirectional rather than vertical fluxes (which have different altitude dependences) [43]. The resulting dataset was normalized as detailed in Appendix A.1 in the Supplementary data. We fit Eq. (2) to the dataset ($n = 113$) with an R^2 value of 0.991 (Fig. 2B, Table 1B and Appendix A.1, Table A1-1B in the Supplementary data). The resulting model should approximate more intermediate solar modulation conditions than the fast-muon model.

We estimated the total uncertainty for the slow-muon model in a similar way to the fast-muon model. The fully propagated model uncertainty in terms of $I_{\mu s}$ ranges from 0.7 to 5% (1σ) up to 6 km altitude. The mean residual in terms of $I_{\mu s}$ was approximately

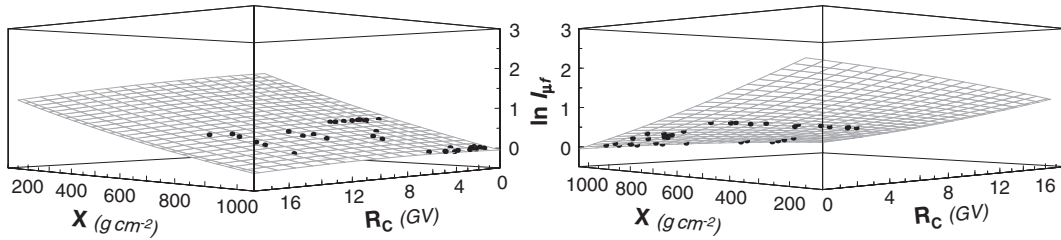
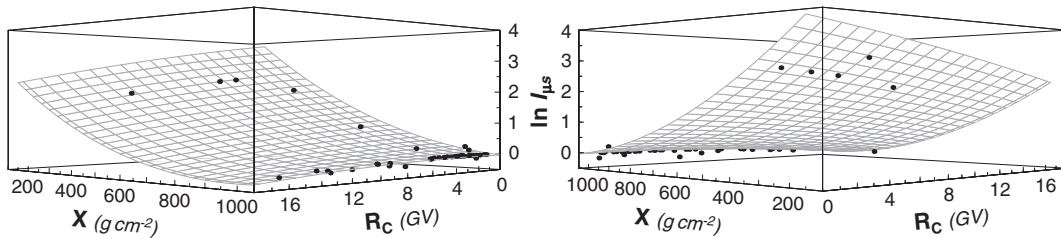
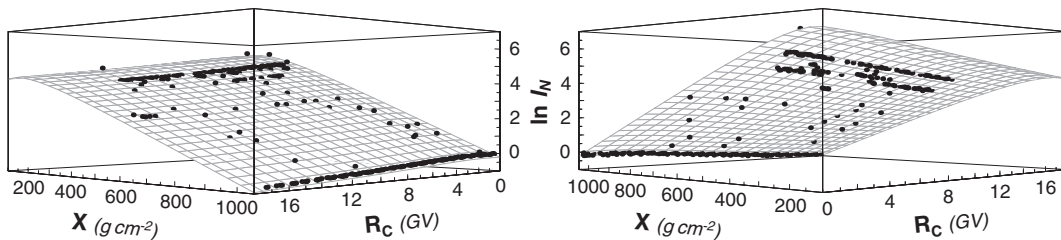
A) FAST MUONS**B) SLOW MUONS****C) SPALLOGENIC NUCLEONS**

Fig. 2. Plots illustrating the fit of our model surfaces to the data (dots) for (A) the fast-muon, (B) the slow-muon, and (C) the spallogenic nucleon scaling models presented here. The surface shown in panel (C) is for an intermediate S value of 0.94. This value was selected for illustrative purposes only—it should not be considered a “best-fit” to the full dataset depicted, since the dataset represents a range of S values. Two perspectives are shown for each opaque surface.

0.6%, with a 1σ of about 6%. We added the 1σ propagated model uncertainty quadratically to the 1σ percentage residual and an assumed additional 6% (1σ ; the midpoint of the range observed by [27]) solar variability for the slow-muon flux, giving a 1σ value ranging from approximately 8 to 10% between sea level and 6 km altitude.

2.2. Spallogenic nucleon scaling model

The spallogenic nucleon scaling model is based on sea level and airborne datasets spanning 5 solar cycles ($n=4618$), covering much of the lower atmo-

sphere and nearly the full range of R_C values currently observed. The model is referenced to neutron monitor data from the oceanic, overland and airborne surveys of Carmichael et al. [39,40] (Appendix A.1 in the Supplementary data). These surveys near the 1965 solar minimum covered X values ranging from 1033 g cm^{-2} to $\sim 200 \text{ g cm}^{-2}$, and R_C values from approximately 0.5 to 13.3 GV. These data were augmented with four other published sea level nucleon intensity surveys conducted at or near solar minima, covering R_C values from 0 to approximately 17.5 GV [52–55]. We should note that Moraal et al.’s [54] original data were not avail-

able (Harm Moraal, personal communication, 1999). We thus used their binned data summary, reducing the impact of that survey on our final dataset.

Solar modulation effects on global high-energy nucleon measurements were addressed by incorporating sea level data from Bieber et al. [10], and airborne data from Sandström [56] (602 g cm^{-2} , 0 to 17.5 GV), Raubenheimer and Stoker [57, and unpublished 1976 data], and unpublished 1976 data] (961 to 307 g cm^{-2} , 3.1 to 14.2 GV), and Stoker and Moraal [22] (475 to 307 g cm^{-2} , 1.4 to 14 GV). The Bieber et al. [10] data were collected between December 1994 and April 2002 as part of an ongoing project to conduct annual sea level neutron monitor latitude surveys over an entire solar cycle. The Sandström [56] data were collected during a period of intermediate solar activity (1957), while the Stoker and Moraal [22] and Raubenheimer and Stoker [57] measurements covered periods of minimum (1966, 1976), intermediate (1971, 1974), and maximum (1969) solar activity.

To combine the disparate surveys into a single, internally consistent dataset, each survey was normalized internally and then scaled relative to the count rates of permanent ground-based neutron monitors at the May 1965 solar minimum. Each survey was subsequently normalized to the Carmichael et al. [39,40] dataset. Each dataset was then corrected for fast- and slow-muon and constant background contributions (due to α particle contamination of the counters [58,59]) to the neutron monitor count rates. Finally, each survey was renormalized to the corrected Carmichael et al. [39,40] dataset. Details of these normalizations and corrections are presented in Appendix A.1 in the Supplementary data.

Two types of neutron monitors were used in the surveys: the IGY and NM-64 designs. Because the NM-64 is sensitive to nucleons of slightly lower median energy (NM-64 ~ 130 MeV vs. IGY ~ 160 MeV) [36], there may be slight differences (2 to 3%) in latitudinal response between the two designs. Comparison of the 1966 (IGY) and 1976 (NM-64) Stoker and Moraal [22] solar minimum data, however, showed no significant difference in latitude effect. Furthermore, Wilson et al. [60] found the responses of IGY and NM-64 monitors to a solar flare event to be indistinguishable. We therefore consider measurement differences resulting from design considerations to be within the uncertainty of the combined dataset (see below).

We based our measure of solar modulation on the variation in monthly mean relative intensity (S) for the two permanent neutron monitors with the longest periods of record (1953 to 2004): Climax and Huancayo/Haleakala ($R_C=2.99$ GV and 12.92 GV, respectively; both at 3.4 km altitude, $X=680 \text{ g cm}^{-2}$) (<ftp://ulysses.sr.unh.edu/NeutronMonitor/DailyAverages.1951–2004.txt>) (Fig. 1). The Huancayo data were corrected for secular drift of the station's R_C value. The Haleakala monitor replaced Huancayo when it closed in late 1992—its count rate is normalized to that of Huancayo [61]. Each S value was calculated relative to the monthly mean intensity at each station during the May 1965 solar minimum, to provide a measure of the relative effect of solar variability at each cutoff [62].

However, neutron monitor count rates lag changes in solar activity due to the propagation time of the solar wind through the heliosphere. We quantified this delay by shifting the mean monthly sunspot number (Z) time series ([63] for 1953 to 1995; ftp://ftp.ngdc.noaa.gov/STP/SOLAR_DATA/SUNSPOT_NUMBERS/MONTHLY for 1996 to 2004) forward in time in 1-month increments from 0 to 20 months, relative to the corresponding time series for the mean monthly intensity of the Climax neutron monitor. For each increment, we calculated the Pearson correlation coefficient and Spearman rank-correlation coefficient between Z and the mean monthly Climax intensity. Results indicate both coefficients are maximized (-0.84 and -0.86 , respectively) for an ~ 8 -month lag time.

We assumed that solar modulation effects on primary intensities are only a function of R_C , based on the findings of [57] and the general formulation of [62] and [64]. We then quantified how neutron monitor count rates vary with solar activity and R_C , by fitting a surface describing the variation of S with R_C and Z (shifted forward 8 months). The resulting fit ($R^2=0.787$; $n=1228$) is based on the formulation of [62] and [64]

$$S = \frac{b_1(R_C - b_2Z)^2}{R_C^{b_3}} \quad (3)$$

where $b_1=(9.8313 \pm 0.0302) \times 10^{-1}$, $b_2=(1.6038 \pm 0.0292) \times 10^{-3}$, $b_3=1.9988 \pm 0.0013$.

We calculated S values for each point in our dataset with Eq. (3) by associating the appropriate shifted Z

with the measurement dates for each survey. S values at $R_C < 3$ GV and > 13 GV were assumed to be the same as the values at those end members. Because Moraal et al. [54] did not include individual survey dates with their summary data, we used the mean shifted Z value during their surveys.

Cosmic ray intensity data have typically been fit at a given altitude or atmospheric depth by one of three types of equations: Dorman functions [15,55], exponential polynomials [22], or sigmoidal functions [28,34]. These functions are then scaled to different altitudes using various models of how A varies with altitude and R_C . Lal [29] took a somewhat different approach, fitting polynomials in altitude to cosmic ray data at given geomagnetic latitudes. Dividing the scaling procedure into two parts reduces the complexity of the fitting problem but, in our view, has disadvantages mentioned earlier.

Nagashima et al. [64] used available neutron monitor surveys to derive energy-dependent neutron monitor responses to solar modulation of the galactic cosmic ray spectrum, as a function of X and R_C . They fitted each survey separately, splitting the problem into three component functions: the unmodulated galactic cosmic ray spectrum, a solar modulation function, and a function describing the yield of neutrons in the atmosphere. They did not correct the survey data for muon or background contributions to the total count rate. While their results agreed reasonably well with theory for high energies (> 10 GeV) at low altitudes, and their model fits some surveys quite well, other results showed significant systematic deviations from both the survey data and theoretical predictions, particularly at higher altitudes.

We took a simpler empirical approach, fitting a 4-dimensional model directly to neutron monitor data collected over a wide range of X and R_C . To do this, we combined a modified Dorman function with an exponential polynomial and incorporated the solar variability through trial and error. Our best-fitting equation ($R^2 = 0.9996$) for relative nucleon intensity (I_N) is

$$\ln(I_N) = c_1 \ln(XS) - Se \left[\frac{c_2 S}{(R_C + 5S)^{2S}} \right] + c_3 X^{c_4} + c_5 [(R_C + 4S)X]^{c_6} + c_7 (R_C + 4S)^{c_8} \quad (4)$$

(Fig. 2C, Table 1C, and Appendix A.1, Table A1-1C in the Supplementary data). Fig. 3 compares three subsets of the data with corresponding model predictions. The fully propagated 1σ model uncertainty in terms of I_N is approximately $< 2\%$ at low R_C values and $< 1\%$ at high R_C values, for long-term S values between 0.84 and 1.02 (assuming a 1σ uncertainty in S of 0.01—approximately the standard error on the relative mean annual Climax intensity). There is no significant dependence of the residuals on X , R_C , or S , indicating that the model adequately describes the measurements. The mean residual for the fit (again in terms of I_N) is approximately 0.4%, with a 4.6% 1σ for the residuals. Although small systematic departures between the model and the data in limited ranges of R_C and X are evident in Fig. 3, they lie within this 1σ range. We therefore use the 1σ propagated model uncertainty added quadratically to the 1σ percentage residual as our time-averaged uncertainty estimate for this model.

Table 1
Scaling model parameter estimates and uncertainties

Parameter	Estimate	Standard Error
<i>A) Fast-muon intensity as $f(R_C, X)$</i>		
a_1	2.4424	1.1848×10^{-1}
a_2	-2.8717×10^{-3}	2.7678×10^{-4}
a_3	4.7441×10^{-7}	1.5923×10^{-7}
a_4	4.3045×10^{-5}	3.2362×10^{-6}
a_5	-3.7891×10^{-2}	3.9933×10^{-3}
a_6	-7.6795×10^{-4}	1.4728×10^{-4}
R^2	0.995	$n = 87$
<i>B) Slow-muon intensity as $f(R_C, X)$</i>		
a_1	5.1132	1.1694×10^{-1}
a_2	-8.8225×10^{-3}	3.8936×10^{-4}
a_3	3.7346×10^{-6}	2.8414×10^{-7}
a_4	7.9712×10^{-5}	8.5686×10^{-6}
a_5	-7.5605×10^{-2}	1.0862×10^{-2}
a_6	-1.3203×10^{-3}	3.8470×10^{-4}
R^2	0.991	$n = 113$
<i>C) Spallogenic nucleon intensity as $f(R_C, X, S)$</i>		
c_1	1.8399	1.0353×10^{-2}
c_2	$-1.1854 \times 10^{+2}$	2.6567
c_3	-4.9420×10^{-2}	1.7512×10^{-3}
c_4	8.0139×10^{-1}	4.2170×10^{-3}
c_5	1.2708×10^{-4}	4.3896×10^{-5}
c_6	9.4647×10^{-1}	3.1630×10^{-2}
c_7	-3.2208×10^{-2}	4.6392×10^{-3}
c_8	1.2688	4.0327×10^{-2}
Nonlinear R^2	0.9996	$n = 4618$

2.3. A model for time-averaged R_C

Model fits are based on essentially instantaneous trajectory-derived R_C values appropriate for when the measurements were made. However, these R_C values change spatially and temporally in response to secular variation of the dipole and non-dipole components of

the geomagnetic field [65–67]. This leads to a problem when attempting to estimate R_C values appropriate for CN applications. It has typically been assumed that secular variation of the geomagnetic pole averages to first order to the geographic pole (i.e., a geocentric axial dipole, or GAD) over a time scale of 10 to 100 ka [18,34,68]. However, this assumption may not be appropriate for Holocene or late Pleistocene samples since eccentric dipole and non-dipole effects may not average to a GAD in that time frame. Furthermore, second-order zonal non-dipole field components (~4% of the dipole field, comparable to modern values) may persist for even longer periods (up to several Ma) [68].

Two models have been proposed to address these issues. Dunai [34] used an approximation for R_C (in GV) based on local records of geomagnetic inclination (i) and the horizontal component of geomagnetic intensity (H , in T) to account for local non-dipole field variations:

$$R_C = \frac{rcH}{4 \times 10^9(1 + 0.25 \tan^2 i)^{1.5}} \quad (5)$$

where r is the radius of the Earth in m and c is the speed of light in m/s. R_C values approximated in this way are incompatible with trajectory-derived values. However, Dunai [69] argued that systematic errors introduced in this approximation should cancel if both modern cosmic ray measurements and paleomagnetic data are ordered with comparable values. Dunai’s [34] model is based on modern cosmic ray

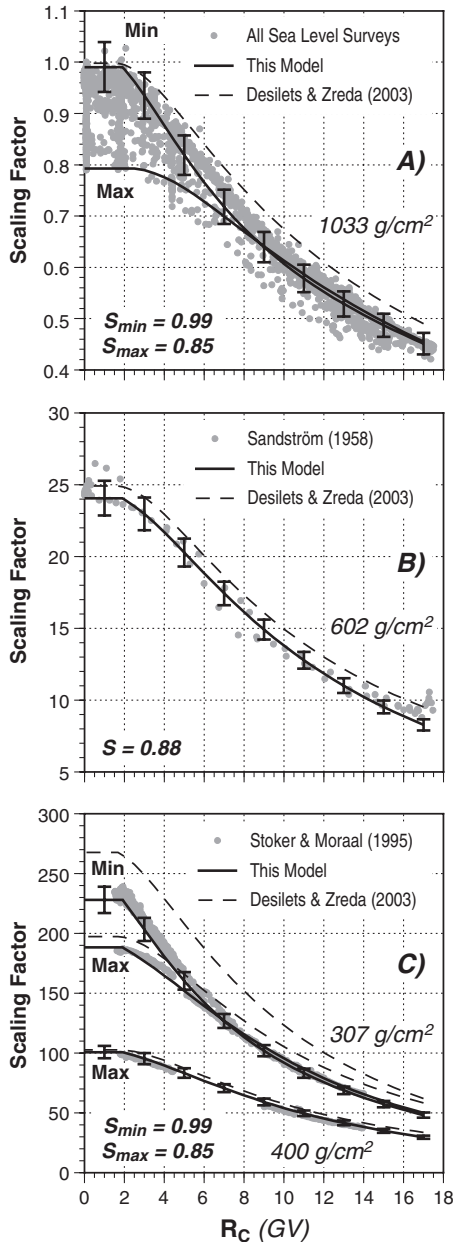


Fig. 3. A comparison of our spallogenic nucleon scaling model predictions and representative subsets of the underlying neutron monitor survey data at different atmospheric depths and solar modulation conditions. The model curves illustrate the range of predictions applicable to each subset of the data. The full dataset used for the model is not depicted. (A) Sea level survey data collected at or near solar minima [39,40,52–55] and from annual sea level surveys from 1994 through 2002 [10]; (B) airborne data from Sandström [56] collected in 1957 at intermediate solar modulation conditions; and (C) airborne 1966 (near solar minimum) and 1969 (near solar maximum) data from [22]. Note the “knee” in each data subset, at $R_C \sim 2$ GV ($\lambda \sim 55^\circ$). Incoming primary cosmic rays with rigidities < 2 GV are still admitted below this R_C , but do not have enough energy to generate secondary cascades that reach the lower atmosphere in significant numbers, and measured spallogenic nucleon intensities remain constant. Indicated uncertainties are 1σ . Also shown for comparison are model predictions of Desilets and Zreda [15].

measurements ordered with Eq. (5), using i and H values derived from detailed geomagnetic field models. However, when applying this parameterization to past geomagnetic variations, one is forced to assume a dipolar representation for H . This can lead to a potential over- or underestimation of the local H of $>50\%$ for the modern geomagnetic field. While one would expect time-integrated magnitudes of such variations in H to be less, the fact that H affects the R_C approximation linearly clearly can lead to significant systematic errors in Dunai's [34] scaling factors.

Desilets and Zreda [15] took a different approach, developing a model based on trajectory-traced R_C values for a GAD field of varying intensity ($R_{C,dpl}$, Eq. (19) of [15]). This approach attempts to bridge the temporal gap between modern trajectory-derived values and trajectory-derived values appropriate for long-term mean geomagnetic conditions [69]. They

also expanded this method to include non-GAD situations in which local paleomagnetic records are available, broadly following [70] and [34]. While these geomagnetic models yield somewhat smaller average and maximum residuals relative to modern trajectory-derived R_C values than Dunai's [34] [15, Table 9], they still do not address potential global non-dipole and eccentric dipole effects which may persist over the Holocene and late Pleistocene.

We propose an alternative model to address these concerns by relating the 5° latitude by 15° longitude world grid of trajectory-derived R_C values for 1955 [14] to geomagnetic latitude (λ). In this model, we use the significant variability in this relationship to derive a long-term λ vs. R_C distribution that averages the effects of the current eccentric dipole and non-dipole fields (\bar{R}_C) (Fig. 4). These data were fit to a cosine function based on the definition of R_C in a geocentric

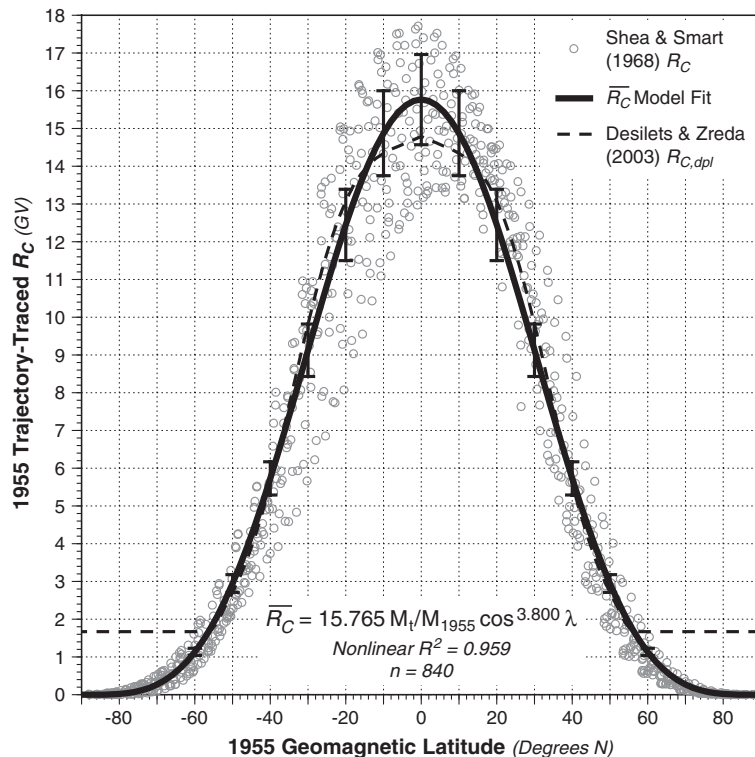


Fig. 4. Plot showing the fit between trajectory-derived R_C [14] and geomagnetic latitude for the 1955.0 DGRF. 1σ uncertainties are shown. The asymmetry of the data reflects the influence of the current eccentric dipole and non-dipole components of the geomagnetic field. Also shown for comparison is the trajectory-traced model of Desilets and Zreda [15], assuming a geocentric axial dipole and a modern geomagnetic intensity.

dipole (not necessarily axial) field [18,21,68] ($R^2=0.959$):

$$\overline{R}_C = d_1 \frac{M_t}{M_{1955}} \cos^{d_2} \lambda \quad (6)$$

where $d_1 = 15.765 \pm 0.093$, $d_2 = 3.800 \pm 0.055$, and M_t/M_{1955} is the dipole intensity at time t relative to that in 1955 (8.050×10^{22} A m², 1955.0 Definitive Geomagnetic Reference Field, or DGRF). The mean residual for the fit is approximately 0.03 GV, with a standard deviation of approximately ± 1.19 GV (1σ). The mean and maximum absolute residuals are 0.8 and 4.2 GV, respectively, comparable to the preferred model of [15, Table 9]. To account for the misfit between individual R_C and \overline{R}_C values, the standard deviation of the mean residual was expressed as a percentage of the equatorial \overline{R}_C value ($\sim 7.55\%$ of d_1), and then added quadratically to the propagated parameter uncertainties. Propagating this total uncertainty through the spallogenic and muogenic models yields maximum 1σ uncertainties ranging between approximately 6 to 11% between sea level and 6 km altitude, respectively, at high \overline{R}_C values.

Our approach is supported by the data of Shea and Smart [65,66], who calculated global trajectory-derived R_C grids at 50-yr intervals between 1600 and 2000 A.D., based on geomagnetic models of at least degree and order 5. Their results indicate that the highest R_C values migrated westward approximately 180° during that period, consistent with accepted secular geomagnetic variations, while the latitudinal R_C distribution remained similar. Our 1955 model agrees within our total 1σ uncertainty with a similar model fit to the entire 1600–2000 dataset. Therefore, using a latitudinally averaged R_C model appears justified for time-integrated applications, based on available data, particularly if realistic uncertainties are included explicitly.

3. Discussion

3.1. Applying the models

To use our models, one must first convert site altitudes to X values. While the U.S. Standard Atmosphere [35] has been commonly used for this purpose,

it was developed to reflect mid-latitude conditions. As such, it deviates from the actual atmospheric structure at high and low latitudes (e.g., Antarctica [3]). Stone [3] and Dunai [28] proposed corrections to the Standard Atmosphere based on observed sea level pressure and temperature values, respectively. Although these corrections do not account for potential corresponding changes in lapse rate or atmospheric structure (e.g., Fig. 8 of [71]), we advocate using the U.S. Standard Atmosphere with appropriate average sea level pressure (e.g., NCEP/NCAR Reanalysis Dataset ds090.2, <http://dss.ucar.edu/datasets/ds090.2/data/monthly/PRES.msl/>) and temperature (e.g., CIRA-86 atmospheric model, <http://nssdc.gsfc.nasa.gov/space/model/atmos/cospar2.html>; see Appendix A.1 in the Supplementary data) values. However, in regions where this model of X vs. altitude might not be appropriate over millennial time scales (e.g., Antarctica [3]), other models for estimating X (with realistic uncertainties) can be substituted.

Pigati and Lifton [2] showed that it is critical to reference variations in geomagnetic intensity and pole position to the present λ of a sampling site (rather than geographic latitude) when accounting for their time-integrated effects on CN production rates, since that is what the sample experiences. Therefore, one should convert geographic latitude to λ (referenced to the 1945.0 DGRF, per [2]) following Merrill et al. [68, Eq. 3.3.8]. Differences between the 1945.0 and 1955.0 DGRFs are not significant for this application, given the uncertainties in \overline{R}_C . This λ value can then be used in Eq. 6 to derive a present-day site \overline{R}_C value to account for temporal geomagnetic variations per Pigati and Lifton [2]. To account for the latitude “knees,” above which the measured intensities remain approximately constant (Appendix A.1 in the Supplementary data), the \overline{R}_C value from for $\lambda=55^\circ$ ($\overline{R}_C = 1.907$ GV) is applied to all $\lambda > 55^\circ$ for the spallogenic model, while an \overline{R}_C value of 4 GV is applied to all $\lambda > 45^\circ$ for the muogenic models.

Finally, one must choose a long-term mean S value, which in practice corresponds to the assumed long-term mean relative Climax neutron monitor intensity (representative of a sea level, low R_C neutron monitor—compare the Climax and Thule neutron monitor records in Fig. 1). Our model is tightly constrained by about 95% of the data between S values of approximately 0.87 to 0.98. Because of the way the neutron

monitor data are normalized, our model should predict sea level, low \bar{R}_C scaling factors that approximate the input S value. In fact, our model yields sea level, low \bar{R}_C scaling factors within 2σ of the input S value for $0.82 < S < 1.13$. Because the model is unconstrained by data for $S > 0.99$, and poorly constrained for $S < 0.85$, it should be robust for $\sim 0.84 < S < \sim 1.00$. Appropriate X , R_C , and S values in (4) and (2) will yield the relative nucleon and fast and slow-muon intensities, respectively, at a given location for those mean solar modulation conditions. Section 3.3 discusses estimating appropriate S values in more detail. To assist the reader in exploring the relationships between long-term solar activity, geomagnetic variability, and scaling factors for CN applications, we include our models in a Microsoft Excel[®] spreadsheet based on that of Pigati and Lifton [2, Appendix 2] as Appendix A.2 in the Supplementary data.

While previous scaling models are normalized to give sea level and low R_C values of 1.0, this model only does that for $S = 1.0$. However, the relative scaling values are correct even if the sea level, low R_C value is not 1. To be internally consistent, calibration sites for production rates should also be scaled to sea level, low R_C values using the same S value and geomagnetic corrections [2] (Appendix A.2 in the Supplementary data).

3.2. Comparison of model predictions

We have attempted to improve on published models for scaling secondary cosmic radiation for in situ CN applications [3,15,28,29,34] by basing our models on significantly more data with wider geographic and temporal coverage. Furthermore, all data on which our spallogenic nucleon model is based are referenced to ground-based monitors at a single time period (the May 1965 solar minimum)—a key improvement over other such models. We focus our discussion, however, on the scaling models of Desilets and Zreda [15] because (1) our parameterizations are similar, allowing direct comparison of our models and datasets (the different latitudinal parameterizations of other models yield systematic deviations from ours), (2) we both subdivide muogenic production into slow and fast (integral) components, and (3) we both include a method to account for solar modulation.

Based on 4618 data points parameterized by R_C , X , and S , we argue that our spallogenic model is more robust and flexible than that of Desilets and Zreda [15]. The data cover nearly the full range of observed R_C values and are evenly distributed between low and high altitudes: $\sim 55\%$ are from X values $> 990 \text{ g cm}^{-2}$ ($< 350 \text{ m}$ altitude), while $\sim 42\%$ are from X values $< 700 \text{ g cm}^{-2}$ ($> 3.2 \text{ km}$ altitude). In contrast, the Carmichael et al. [39,40] dataset upon which [15] based their model contains only 110 measurements: 50 are from $> 990 \text{ g cm}^{-2}$, while only 25 points are from $< 700 \text{ g cm}^{-2}$. While strongly weighted to data from high altitudes and sea level, our model yields A values which are entirely consistent with those of both [15] and [34] within their stated uncertainties. Data used in our model are as evenly distributed as possible (given available sources) among various portions of the solar cycle. Approximately 48% of the data are from solar minimum or near-solar-minimum periods, while the other 52% are distributed through solar maximum and intermediate periods. Furthermore, compared to the muon scaling models presented by [15], our fast-muon model is based on 34% more data from high altitudes, and our slow-muon model is based on 5 times the data from $R_C \geq 14 \text{ GV}$ (5 measurements vs. 1).

Comparisons of our model predictions with those of [15] are presented in Fig. 3 with subsets of our underlying data, and in Fig. 5 for our respective time-integrated R_C models. Fig. 3A demonstrates the importance of normalizing all data to a single reference time. While both our spallogenic nucleon model and that of [15] are based on the [39,40] dataset, [15] do not account for absolute differences in intensity between their preferred sea level survey from 1997 [11,55] and the May 1965 datum of [39,40]. The result is that [15] predicts sea level intensities for $R_C > 2 \text{ GV}$ which are systematically higher than the trend in our composite solar minimum sea level dataset. On the other hand, our model tends to underestimate the trend in the solar minimum data at sea level for $\sim 4 < R_C < \sim 10 \text{ GV}$, but does so within our stated uncertainty. Desilets and Zreda [15] quote no uncertainty for their sea level intensity-vs.- R_C function, although [11] give the uncertainties in the parameters as $\sim 0.2\%$.

Another significant issue is that while [15] includes a formula to accommodate solar modulation in A for spallogenic nucleons, they lack a corresponding mechanism to modulate their sea level intensity-vs.-

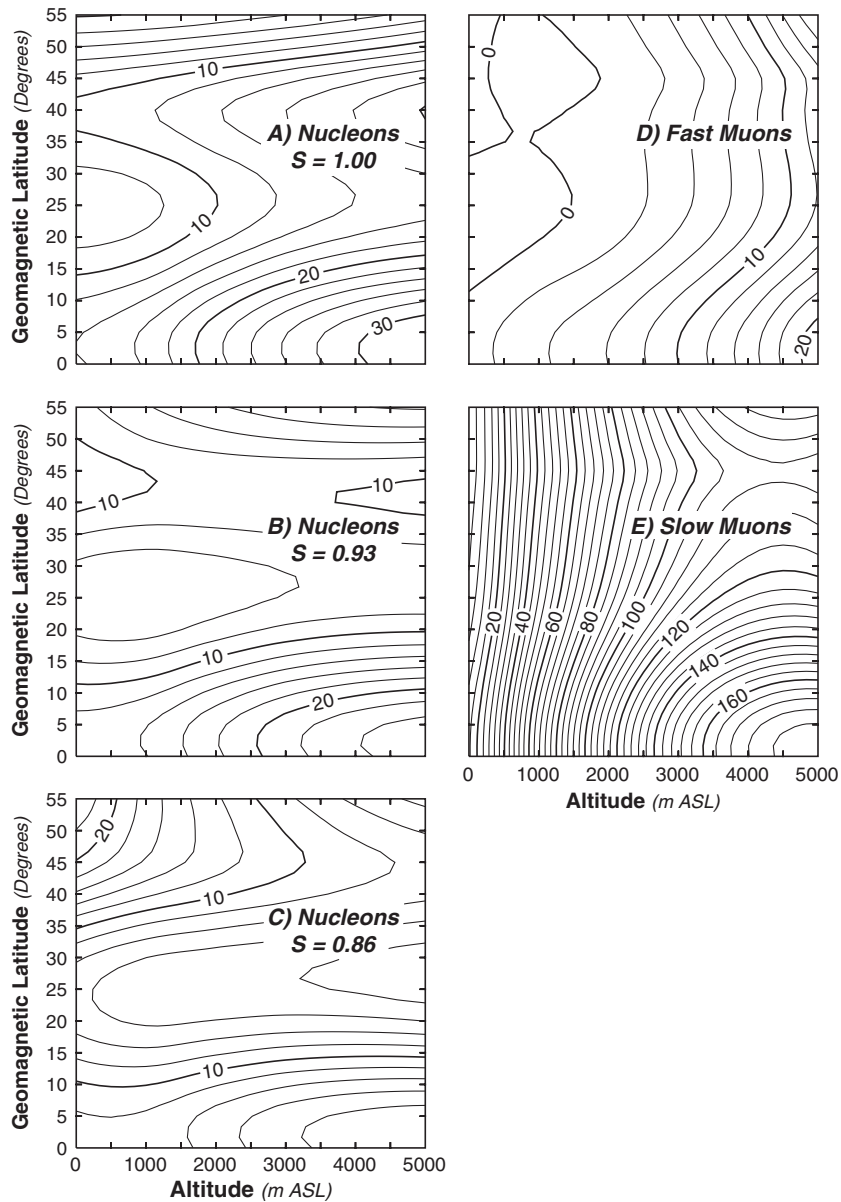


Fig. 5. Percentage differences between the spallogenic nucleon (A, B, C) and muogenic (D, E) scaling models of Desilets and Zreda [15] and those presented here. For the spallogenic nucleon models, differences at high latitudes reflect the fact that the Desilets and Zreda [15] model does not allow for sea level variation of nucleon intensity. Low latitude differences in our scaling models reflect contrasts between our long-term R_C model and that of [15]. Contour interval is 2% for panels (A–D), and 4% for panel (E).

R_C curve. This is evident in Fig. 3B and C, in which the systematic offset at sea level is propagated upward through the atmosphere. The offset improves somewhat at 400 g cm^{-2} , due to the manner in which A varies with X and R_C in their model, but worsens

significantly by 307 g cm^{-2} . In comparison, our model fits the data reasonably well for a wide range of solar modulation conditions over the entire altitude range considered, although small deviations are present within our stated uncertainty.

We also compared our models to those of [15] using our respective time-integrated R_C models (\bar{R}_C vs. $R_{C,dpl}$) for S values of 1.0, 0.93, and 0.86. Observed differences between the spallogenic models are greatest at low λ values during solar minima, at high λ values during solar maxima, and are generally comparable at high and low λ values at intermediate solar activity levels. For high and intermediate solar activity, these differences tend to diminish with increasing altitude at high λ values, but remain relatively constant with altitude during solar minima. At low λ values, differences increase with increasing altitude for all solar activity levels.

Both models only agree within our 1σ uncertainty for $S=1.0$ at high λ values between 0 and 5 km altitude. We do not propagate the uncertainty for [15] here, since its exponential growth with increasing altitude seems unrealistic. With increasing solar activity, however, the models agree within 1σ only at $\lambda=55^\circ$ between 2 and 5 km altitude, and for $20^\circ < \lambda < 30^\circ$ from 0 to 5 km. High- and mid-latitude differences tend to grow at low altitudes with increasing solar activity, until at $S=0.86$, [15] predict scaling factors ranging up to $\sim 25\%$ greater than ours. This increasing discrepancy with increasing solar activity reflects the fact that their sea level latitude curve does not vary with solar activity levels. At low latitudes, Desilets and Zreda [15] predict spallogenic scaling factors that are 10 to 30% greater than ours, decreasing slightly with decreasing S , reflecting our different approaches to modeling long-term R_C . At the 2σ level, for $S=1.0$ the models disagree at mid- λ values and altitudes >1 km, and at low λ values. With increasing solar activity, the models generally agree at 2σ , except for low λ values and >1 km altitude ($S=0.93$) and $\lambda > 40^\circ$ and < 3 km altitude ($S=0.86$), emphasizing the aforementioned differences.

Our fast-muon model generally agrees within our stated uncertainties with that of Desilets and Zreda [15] below 2 to 3 km altitudes, while their fast-muon model yields scaling factors $>10\%$ above ours at 4 to 5 km. Our slow-muon models agree within uncertainties near sea level, but diverge rapidly with altitude—Desilets and Zreda [15] predict slow-muon scaling factors from ~ 50 to 160% higher than ours between 2 and 5 km. Thus, significant differences exist between our scaling models and those of Desilets and Zreda [15], particularly at high and low geomagnetic latitudes.

3.3. Estimating long-term mean solar modulation conditions

Fig. 3 indicates that S values ranging from 0.99 to 0.85 reasonably describe the overall trends in the solar minimum and maximum datasets, respectively, at altitudes from sea level to 9.1 km (1033 to 307 g cm $^{-2}$). Unfortunately, estimating a long-term mean solar modulation value appropriate for CN applications is not so straightforward. Observations of sunspot numbers only extend back to the early 17th century [63], while various proxy methods have been used for estimating solar variability beyond the instrumental record (e.g., [19,31,72–79]).

Atmospheric cosmogenic nuclides such as ^{14}C and ^{10}Be are useful for studying long-term solar variability, since they are retained in natural archives such as tree rings and ice caps. Significant progress has been made recently in relating atmospheric ^{14}C and ^{10}Be production rates from proxy records both to solar influences and to instrumental cosmic ray measurements (e.g., [79–84]). The annually-resolved record of ^{14}C activities in tree rings extends back to ~ 11.4 ka, but this globally averaged signal is tied to the carbon cycle and requires a box model to interpret atmospheric ^{14}C production variations (e.g., [85]). Meteoric (not in situ) ^{10}Be in polar ice caps is attractive for constraining past solar behavior, since it has a short (~ 1 yr) atmospheric residence time and long records exist with near-annual (e.g., Dye-3 from Greenland [86]) to sub-decadal resolution (e.g., SP-1 from Antarctica [76]). Furthermore, approximately 70% of the polar ^{10}Be signal is produced at high geomagnetic latitudes, making these records sensitive to solar effects [87,88]. However, the records are currently discontinuous through the Holocene, and problems arise in attempting to relate them quantitatively. We therefore prefer the tree-ring ^{14}C record over the ^{10}Be concentration in polar ice as a basis for estimating long-term relative neutron monitor intensities.

Solanki et al. [79] used the tree-ring-derived ^{14}C production rate record of [85] and a series of physics-based models to reconstruct 10-yr averaged sunspot numbers over the last 11.4 ka. However, Pigati and Lifton [2] used 100-yr time steps for their analysis of geomagnetic fluctuations, upon which we base our Appendix A.2 in the Supplementary data. We therefore used 100-yr weighted mean sunspot numbers

from [79] as input to Eq. (3) to derive a corresponding record for S , assuming $R_C < 3$ GV (Appendix A.2 in the Supplementary data).

The weighted mean S value for the last 11.4 ka is 0.950, with individual 100-yr mean values ranging from 0.906 to 0.977. For comparison, S values derived from the original 10-yr averaged data of [79] yielded a weighted mean of 0.959, and ranged from 0.876 to 0.984. While this range is similar to that derived from mean annual Climax relative intensity (1953–2004, referenced to May 1965), the weighted mean is somewhat higher than the mean Climax value (0.923), reflecting unusually high solar activity level over the last 70 yr [79]. While the 100-yr mean variability is attenuated relative to that of the 10-yr mean record, however, it should still be appropriate for our purposes since solar effects on measured CN concentrations are time-integrated. Clearly, though, more work is needed to understand millennial-scale variability in solar modulation (e.g., [81,82]).

3.4. Applying secondary cosmic ray scaling models to *in situ* cosmogenic nuclides

We have demonstrated that our models for scaling spallogenic nucleons and both fast and slow muons in the lower atmosphere can reasonably account for the effects of solar modulation on those secondary cosmic ray components. However, applying these models to scaling terrestrial CN production rates requires consideration of integrated differences between the energy-dependent responses of both the instruments and the CNs to solar modulation of the incident cosmic ray spectrum (e.g., [13,15,20,25,69]). These differences vary according to the excitation function for each relevant reaction (the probability of nuclide production as a function of incident particle energy for a given target atom) [20].

Unfortunately, key data needed to evaluate these differences quantitatively are presently limited at best. For example, excitation functions for spallogenic neutron production of most commonly used CNs have not yet been measured directly (these are often extrapolated from measured proton excitation functions, e.g., [89,90]). Furthermore, measured neutron differential spectra (change in flux or intensity as a function of energy) available for the lower atmosphere generally only represent intermediate conditions [91–94]. Gor-

don et al. [91] suggest that for neutron energies > 5 MeV, the shape of the ground-level spectrum does not change significantly with solar modulation, at least for $R_C < 5$ GV and $1033 < X < 680$ g cm⁻² (< 3.4 km altitude). O'Brien et al. [95] argued that this is a reasonable scenario for neutron energies < 100 MeV, while model neutron spectra for sea level and $R_C = 0$ GV from Masarik and Beer [96] support this hypothesis for energies $< \sim 300$ to 400 MeV. However, this is counterintuitive, since the shape of the *primary* spectrum changes markedly during a solar cycle (e.g., [97,98]). In fact, analyses of neutron monitor responses to solar modulation are typically cast in terms of the primary spectrum, reflecting the magnitude of the spectral modulation at particle rigidities < 10 GV [37,64,98]. Moreover, measured changes in neutron monitor A values over a solar cycle indicate corresponding variations in the shape of the neutron spectrum incident on the monitors [23,26]. This is supported by measurements of 1–10 MeV neutrons near solar minimum and maximum in 1965 and 1969, respectively, which indicate low- R_C variations at 700 g cm⁻² on the order of 30% [99]. Therefore, further measurements and/or modeling are needed to document the effects of solar modulation on the ground-level neutron spectrum.

We can, however, qualitatively assess the dependence of CN production on solar modulation at this time. Solar modulation of the primary spectrum increases with decreasing particle rigidity (particularly < 1 GV)—in theory, this should lead to a corresponding effect in the atmosphere. The degree to which modulation affects a given CN production rate thus depends on how much the excitation functions for that nuclide emphasize production at lower energies. A simple measure of that emphasis is the median energy for production, calculated by integrating the product of the CN excitation function for a given reaction with an incident neutron differential spectrum [15]. A similar calculation can be done for neutron monitors [36]. Neutron monitors have median energies ~ 140 MeV, as does ¹⁰Be for its dominant neutron-induced reaction in silicates (e.g., [15]). The ³He median energy may be > 100 MeV as well [69], but its neutron excitation functions are not well-known. On the other hand, [15, and D. Desilets, 2005, personal communication] calculate median energies of ~ 60 to 70 MeV for ²⁶Al and ¹⁴C (and ³⁶Cl from Ca) from similar

reactions, while ^{36}Cl from K has a median energy on the order of 10 MeV. As the difference between CN and neutron monitor median energies increases, the proportionality between neutron monitor and CN scaling factors may need increasing modification [15].

If we assume that Gordon et al. [91] are correct in that the neutron spectral shape does not change significantly with solar modulation near the Earth's surface, then we need only consider the potential scaling model modifications described above. However, if the shape of the ground-level neutron spectrum varies significantly with solar activity, then we must also account for corresponding relative changes in the median energies of both neutron monitors and CN production reactions of interest. Interaction of the spectral changes with the various CN excitation functions and neutron monitor detection efficiency [37] could cause the relative differences in their median energies to increase, decrease or remain the same. We therefore view developing a better understanding of how the ground-level neutron spectrum responds to solar modulation of the primary flux as a critical topic for future research.

4. Conclusions

Variations in solar activity have the greatest effect on in situ CN production rates precisely at the high λ (low R_C) locations to which those production rates are traditionally referenced. This issue is most significant when scaling intensities (and CN production rates) from high to moderate R_C values (minimally affected by solar modulation) to low R_C values (significantly affected by solar modulation), or vice-versa. Many CN production rate calibration sites are located at moderate or high R_C values (e.g., [100–109]), but resulting production rates are typically scaled to a sea level and low R_C reference location. However, solar variation should not significantly affect scaling between sites which are each at high or moderate R_C values ($>\sim 5$ to 6 GV).

Short-term fluctuations in solar modulation of primary cosmic rays are of little consequence to in situ CNs commonly used in geomorphic studies, since these fluctuations are averaged throughout a sample's exposure history. Short-term fluctuations do, however, affect the cosmic ray measurements on which all CN scaling models have been based. Furthermore, the

temporally averaged modulation level is currently uncertain, but can have important implications for in situ CN production rate scaling. In addition, significant uncertainties exist in applying proposed approximations of geomagnetic effects on CN scaling over millennial time scales.

We have addressed these uncertainties with a spallogenic nucleon scaling model utilizing data distributed over 5 solar cycles that explicitly incorporates a measure of solar modulation, and fast- and slow-muon scaling models (based on more limited data) that account for solar modulation effects through increased uncertainties. Our models improve on previously published models by incorporating significantly more data from a wider time range—better sampling the observed variability in measured cosmic ray intensities as a function of geomagnetic latitude, altitude, and solar activity. Furthermore, placing the spallogenic nucleon data in a common time-space framework allows for a more realistic assessment of uncertainties in our model than in previous ones. We have also proposed a model for time-averaged R_C that explicitly incorporates a realistic level of uncertainty.

We have demonstrated that our models reasonably account for the effects of solar modulation on measured cosmic ray intensities, within the uncertainties of each of our composite datasets. Moreover, our time-averaged geomagnetic model is consistent with the average R_C configuration over the last 400 yr. The spallogenic nucleon scaling model of Desilets and Zreda [15] predicts scaling factors ranging up to $\sim 30\%$ above those of our spallogenic model, while their muogenic scaling models predict scaling factors up to 160% greater than ours. Furthermore, estimates of solar modulation conditions based on a sunspot number reconstruction derived from tree-ring ^{14}C data suggest spallogenic scaling factors in our model for sea level and high geomagnetic latitudes can differ by up to $\sim 10\%$, depending on the time step over which the modulation conditions are averaged. The potential magnitude of this difference supports the argument for incorporating long-term solar modulation into CN production rate scaling. However, more work is needed toward understanding the mean solar modulation conditions over millennial time scales.

In situ cosmogenic ^{14}C (in situ ^{14}C) holds promise in this regard. Due to its short half-life (5.73 ka), in

situ ^{14}C reaches a secular equilibrium between production and decay after ~ 25 kyr of exposure. Secular equilibrium concentrations are only a function of the long-term mean production rate and the decay constant. Thus, by measuring in situ ^{14}C concentrations in geomorphic surfaces that are at secular equilibrium, from a wide range of altitudes and latitudes, we should be able to estimate time-integrated production rates. If differences in energy response of ^{14}C production and neutron monitors can be accounted for, long-term mean S values could then be estimated with our model. This work is in progress and will be fully presented and explored in a future paper. Until then, we believe our S value record for the last 11.4 ka. (Appendix A.2 in the Supplementary data) is reasonable for scaling spallogenic nucleons during that time frame, and that the weighted mean S value of 0.950 is appropriate for longer exposure times.

Our results also highlight several key future research directions. It is difficult to quantify the effects of solar modulation on CN production by nucleon spallation without accurate neutron spectra for both solar maximum and solar minimum conditions. Better characterization of solar modulation effects on the ground-level neutron spectrum and measurement of excitation functions for spallogenic neutron-induced reactions are thus critical topics for future CN research. This will enable quantitative assessment of the degree to which neutron monitors are appropriate for scaling various spallogenic nuclides [15,69]. Furthermore, how best to address past geomagnetic variability in CN scaling models remains an open question. Finally, further research to develop more robust representations of the atmospheric structure for CN applications is also warranted.

Acknowledgements

The authors would like to acknowledge funding from NSF Grant EAR-0001069 and the NSF-Arizona Accelerator Mass Spectrometry Facility to Lifton, NSF Grant ATM-0000315 to the Bartol Research Institute at the University of Delaware, and NSF Grant ATM-9912341 to the University of Chicago for the Climax and Huancayo neutron monitor data. The authors wish to thank Pieter Stoker and Christo Raubenheimer for providing the published 1965–76

airborne neutron monitor survey data, as well as an unpublished altitude survey from 1976. We also thank M.A. Shea and D.F. Smart for providing the global R_C grids for 1600–2000, Sami Solanki for providing the ^{14}C -derived sunspot reconstruction, and Jozef Masarik for furnishing model ground-level neutron spectra. This research benefited greatly from discussions with Jeff Pigati, Tim Shanahan and Darin Desilets. We would like to thank Devendra Lal and Tibor Dunai for the constructive and helpful reviews. Jeff Pigati also provided constructive reviews of various versions of this manuscript.

Appendix A. Supplementary data

Supplementary data associated with this article can be found, in the online version, at [doi:10.1016/j.epsl.2005.07.001](https://doi.org/10.1016/j.epsl.2005.07.001).

References

- [1] T.K. Gaisser, *Cosmic Rays and Particle Physics*, Cambridge University Press, Cambridge, UK, 1990, 279 pp.
- [2] J.S. Pigati, N.A. Lifton, Geomagnetic effects on time-integrated cosmogenic nuclide production with emphasis on in-situ ^{14}C and ^{10}Be , *Earth Planet. Sci. Lett.* 226 (2004) 193–205.
- [3] J.O. Stone, Air pressure and cosmogenic isotope production, *J. Geophys. Res.* 105 (2000) 23753–23759.
- [4] P.E. Damon, C.P. Sonnett, Solar and terrestrial components of the atmospheric ^{14}C variation spectrum, in: C.P. Sonnett, M.S. Giampapa, M.S. Matthews (Eds.), *The Sun in Time*, The University of Arizona Press, Tucson, AZ, 1991, pp. 360–388.
- [5] R.C. Reedy, J.R. Arnold, D. Lal, Cosmic-ray record in solar system matter, *Science* 219 (1983) 127–135.
- [6] D.J. Cooke, J.E. Humble, M.A. Shea, D.F. Smart, N. Lund, I.L. Rasmussen, B. Byrnak, P. Goret, N. Petrou, On cosmic-ray cut-off terminology, *Nuovo Cim., Ser. C* 14 (1991) 213–234.
- [7] O.C. Allkofer, P.K.F. Grieder, Cosmic rays on Earth, *Phys. Data* 25 (1984) 1–379.
- [8] M.A. Shea, D.F. Smart, K.G. McCracken, A study of vertical cutoff rigidities using sixth degree simulations of the geomagnetic field, *J. Geophys. Res.* 70 (1965) 4117–4130.
- [9] J.M. Clem, J.W. Bieber, M. Duldig, P. Evenson, D. Hall, J. Humble, Contribution of obliquely incident particles to neutron counting rate, *J. Geophys. Res.* 102 (1997) 26919–26926.
- [10] J.W. Bieber, J.M. Clem, M. Duldig, P. Evenson, J. Humble, R. Pyle, Cosmic ray spectra and the solar magnetic polarity:

- preliminary results from 1994–2002, in: M. Velli, R. Bruno, F. Malara (Eds.), *Solar Wind Ten: Proceedings of the Tenth International Solar Wind Conference*, Astronomy and Astrophysics, vol. 679, American Institute of Physics, Pisa, Italy, 2003, pp. 628–631.
- [11] L.I. Dorman, G. Villaresi, N. Iucci, M. Parisi, M.I. Tyasto, O.A. Danilova, N.G. Ptitsyna, Cosmic ray survey to Antarctica and coupling functions for neutron component near solar minimum (1996–1997): 3. Geomagnetic effects and coupling functions, *J. Geophys. Res.* 105 (2000) 21047–21056.
- [12] M.A. Shea, D.F. Smart, E.O. Flückiger, Magnetospheric models and trajectory computations, *Space Sci. Rev.* 93 (2000) 305–333.
- [13] D. Desilets, M.G. Zreda, N.A. Lifton, Comment on “Scaling factors for production rates of in situ produced cosmogenic nuclides: a critical reevaluation” by Tibor J. Dunai, *Earth Planet. Sci. Lett.* 188 (2001) 283–287.
- [14] M.A. Shea, D.F. Smart, J.R. McCall, A five degree by fifteen degree world grid of trajectory-determined vertical cutoff rigidities, *Can. J. Phys.* 46 (1968) S1098–S1101.
- [15] D. Desilets, M.G. Zreda, Spatial and temporal distribution of secondary cosmic-ray nucleon intensities and applications to in situ cosmogenic dating, *Earth Planet. Sci. Lett.* 206 (2003) 21–42.
- [16] J.F. Ziegler, Terrestrial cosmic ray intensities, *IBM J. Res. Develop.* 42 (1998) 117–140.
- [17] J.E. Keith, R.W. Peterson, R.L. Tjonaman, J.R. Wang, Cosmic-ray neutron monitor yield functions, Gross transformation, and nucleonic component mean free paths, *J. Geophys. Res.* 73 (1968) 353–360.
- [18] J.C. Gosse, F.M. Phillips, Terrestrial in situ cosmogenic nuclides: theory and application, *Quat. Sci. Rev.* 20 (2001) 1475–1560.
- [19] A.N. Peristykh, P.E. Damon, Persistence of the Gleissberg 88-year solar cycle over the last $\approx 12,000$ years: evidence from cosmogenic isotopes, *J. Geophys. Res.* 108 (2003) 1003, doi:10.1029/2002JA009390.
- [20] D. Lal, B. Peters, Cosmic ray produced radioactivity on the Earth, in: K. Sitte (Ed.), *Handbuch Der Physik XLVI/2*, Springer-Verlag, Berlin, 1967, pp. 551–612.
- [21] D. Lal, Theoretically expected variations in the terrestrial cosmic ray production rates of isotopes, in: G.C. Castagnoli (Ed.), *Proceedings of the Enrico Fermi International School of Physics*, vol. 95, Italian Physical Society, Varenna, 1988, pp. 216–233.
- [22] P.H. Stoker, H. Moraal, Neutron monitor latitude surveys at aircraft altitudes, *Astrophys. Space Sci.* 230 (1995) 365–373.
- [23] F. Bachelet, E. Dyring, N. Iucci, G. Villaresi, Synoptic study of the attenuation coefficients for the cosmic-ray neutron monitors of the IGY network from 1957 to 1965, *Nuovo Cim.* 52B (1967) 106–123.
- [24] D.W. Kent, M.A. Pomerantz, Cosmic ray intensity variations in the lower atmosphere, *J. Geophys. Res.* 76 (1971) 1652–1661.
- [25] D. Desilets, M.G. Zreda, On scaling cosmogenic production rates for altitude and latitude using cosmic-ray measurements, *Earth Planet. Sci. Lett.* 193 (2001) 213–225.
- [26] F. Bachelet, N. Iucci, G. Villaresi, N. Zangrilli, The cosmic-ray spectral modulation above 2 GV: IV. The influence on the attenuation coefficient of the nucleonic component, *Nuovo Cim.* 11B (1972) 1–12.
- [27] O.C. Allkofer, H. Jokisch, A survey on the recent measurements of the absolute vertical cosmic-ray muon flux at sea level, *Nuovo Cim.* 15A (1973) 371–389.
- [28] T.J. Dunai, Scaling factors for production rates of in situ produced cosmogenic nuclides: a critical reevaluation, *Earth Planet. Sci. Lett.* 176 (2000) 157–169.
- [29] D. Lal, Cosmic ray labeling of erosion surfaces: in situ nuclide production rates and erosion models, *Earth Planet. Sci. Lett.* 104 (1991) 424–439.
- [30] I.G. Usoskin, K. Mursula, Long-term solar cycle evolution: review of recent developments, *Sol. Phys.* 218 (2003) 319–343.
- [31] D.J. Schove, The sunspot cycle, 649 B.C. to A.D. 2000, *J. Geophys. Res.* 60 (1955) 127–146.
- [32] R.C. Reedy, K. Marti, Solar-cosmic-ray fluxes during the last ten million years, in: C.P. Sonnett, M.S. Giampapa, M.S. Matthews (Eds.), *The Sun in Time*, The University of Arizona Press, Tucson, AZ, 1991, pp. 260–287.
- [33] D. Lal, Investigations of nuclear interactions produced by cosmic rays, PhD dissertation, Bombay University (1958).
- [34] T.J. Dunai, Influence of secular variation of the geomagnetic field on production rates of in situ produced cosmogenic nuclides, *Earth Planet. Sci. Lett.* 193 (2001) 197–212.
- [35] National Oceanic and Atmospheric Administration, National Aeronautics and Space Administration, United States Air Force, U.S. Standard Atmosphere, Washington, DC (1976) 227 pp.
- [36] C.J. Hatton, The neutron monitor, *Prog. Elem. Part. Cosm. Ray Phys.* 10 (1971) 3–100.
- [37] J.M. Clem, L.I. Dorman, Neutron monitor response functions, *Space Sci. Rev.* 93 (2000) 335–359.
- [38] P.R. Bevington, D.K. Robinson, *Data Reduction and Error Analysis for the Physical Sciences*, McGraw-Hill, New York, NY, 1992, 328 pp.
- [39] H. Carmichael, M. Bercovitch, J.F. Steljes, M. Magidin, I. Cosmic-ray latitude survey in North America in summer, 1965, *Can. J. Phys.* 47 (1969) 2037–2050.
- [40] H. Carmichael, M.A. Shea, R.W. Peterson III, Cosmic-ray latitude survey in Western USA and Hawaii in summer, 1966, *Can. J. Phys.* 47 (1969) 2057–2065.
- [41] A.K. De, P. Ghosh, A.K. Das, Latitude effect of the low momentum muon spectrum at sea level, *J. Phys. A: Math. Nucl. Gen. Phys.* 7 (1974) 150–157.
- [42] W.L. Kraushaar, Cosmic-ray mesons near sea level, *Phys. Rev.* 76 (1949) 1045–1058.
- [43] M. Conversi, Experiments on cosmic-ray mesons and protons at several altitudes and latitudes, *Phys. Rev., Ser. A* 79 (1950) 749–767.
- [44] O.C. Allkofer, K. Clausen, W.D. Dau, The low-momentum muon spectrum near the equator, *Lett. Nuovo Cimento* 12 (1975) 107–110.

- [45] M.P. de Pascale, A. Morselli, P. Picozza, R.L. Golden, C. Grimani, B.L. Kimbell, S.A. Stephens, S.J. Stochaj, W.R. Webber, G. Basini, F. Bongiorno, F.M. Brancaccio, M. Ricci, J.F. Ormes, E.S. Seo, R.E. Streitmatter, P. Papini, P. Spillantini, M.T. Brunetti, A. Codino, M. Menichelli, I. Salvatori, Absolute spectrum and charge ratio of cosmic ray muons in the energy region from 0.2 GeV to 100 GeV at 600 m above sea level, *J. Geophys. Res.* 98 (1993) 3501–3507.
- [46] B. Baschiera, G. Basini, H. Bilokon, B. d’Ettorre Piazzoli, G. Mannocchi, C. Castagnoli, P. Picchi, Integral and differential absolute intensity measurements of cosmic-ray muons below 1 GeV, *Nuovo Cim.* 2C (1979) 473–487.
- [47] L. Del Rosario, J. Dávila-Aponte, Range distribution of sea-level mesons at low geomagnetic latitudes, *Phys. Rev.* 88 (1952) 998–1002.
- [48] S.K. Jain, Vertical cosmic ray muon flux and charge ratio in the momentum region (0.3 GeV/c–2 GeV/c), *Proc. Indian Acad. Sci.* 46A (1980) 149–157.
- [49] B.C. Rastin, An accurate measurement of the sea-level muon spectrum within the range 4 to 3000 GeV/c, *J. Phys., G, Nucl. Phys.* 10 (1984) 1609–1628.
- [50] A. Subramanian, S. Naranan, P.V. Ramanamurthy, A.B. Sahiar, S. Lal, Flux of slow μ -mesons and protons near the geomagnetic equator, *Nuovo Cim.* 7 (1958) 110–113.
- [51] M. Sands, Low energy mesons in the atmosphere, *Phys. Rev.* 77 (1950) 180–193.
- [52] D.C. Rose, K.B. Fenton, J. Katzman, J.A. Simpson, Latitude effect of the cosmic ray nucleon and meson components at sea level from the Arctic to the Antarctic, *Can. J. Phys.* 34 (1956) 968–984.
- [53] M.S. Potgieter, B.C. Raubenheimer, P.H. Stoker, A.J. van der Walt, Modulation of cosmic rays during solar minimum: Part 2. Cosmic ray latitude distribution at sea-level during 1976, *S. Afr. J. Phys.* 3 (1980) 77–89.
- [54] H. Moraal, M.S. Potgieter, P.H. Stoker, A.J. Van der Walt, Neutron monitor latitude survey of cosmic ray intensity during the 1986/1987 solar minimum, *J. Geophys. Res.* 94 (1989) 1459–1464.
- [55] G. Villaresi, L.I. Dorman, N. Iucci, N.G. Ptitsyna, Cosmic ray survey to Antarctica and coupling functions for neutron component near solar minimum (1996–1997): 1. Methodology and data quality assurance, *J. Geophys. Res.* 105 (2000) 21025–21034.
- [56] A.E. Sandström, Cosmic ray soft component measurements during a flight from Scandinavia across the North Pole and around Asia and Europe, *Nuovo Cim., Suppl.* 8 (Series 10) (1958) 263–276.
- [57] B.C. Raubenheimer, P.H. Stoker, Various aspects of the attenuation coefficient of a neutron monitor, *J. Geophys. Res.* 79 (1974) 5069–5076.
- [58] I.L. Fowler, Very large boron trifluoride proportional counters, *Rev. Sci. Instrum.* 34 (1963) 731.
- [59] H. Carmichael, M. Bercovitch, V. Analysis of IQSY cosmic-ray survey measurements, *Can. J. Phys.* 47 (1969) 2073–2093.
- [60] B.G. Wilson, T. Mathews, R.H. Johnson, Intercomparison of neutron monitors during solar flare increases, *Phys. Rev. Lett.* 18 (1967) 675–676.
- [61] R. Pyle, The Haleakala cosmic ray neutron monitor station: intercalibration with the Huancayo station, 23rd International Cosmic Ray Conference 3, Calgary, Alberta, Canada, 1993, p. 609.
- [62] J.W. Bieber, J.M. Clem, M. Duldig, P. Evenson, J. Humble, R. Pyle, A continuing yearly neutron monitor latitude survey: preliminary results from 1994–2001, in: W. Droege, H. Kunow, M. Scholer (Eds.), 27th International Cosmic-Ray Conference Solar and Heliospheric Phenomena, Hamburg, Germany, 2001, pp. 4087–4089.
- [63] D.V. Hoyt, K.H. Schatten, Group sunspot numbers: a new solar activity reconstruction, *Sol. Phys.* 179 (1998) 189–219.
- [64] K. Nagashima, S. Sakakibara, K. Murakami, I. Morishita, Response and yield functions of neutron monitor, galactic cosmic-ray spectrum and its solar modulation, derived from all the available world-wide surveys, *Nuovo Cim.* 12C (1989) 173–209.
- [65] M.A. Shea, D.F. Smart, Preliminary study of cosmic rays, geomagnetic field changes and possible climate changes, *Adv. Space Res.* 34 (2004) 420–425.
- [66] D.F. Smart, M.A. Shea, Geomagnetic cutoff rigidity calculations at 50-year intervals between 1600 and 2000, in: T. Kajita, Y. Asaoka, A. Kawachi, Y. Matsubara, M. Sasaki (Eds.), 28th International Cosmic Ray Conference, Universal Academy Press, Tsukuba, Japan, 2003, pp. 4201–4204.
- [67] A. Bhattacharyya, B. Mitra, Changes in cosmic ray cut-off rigidities due to secular variations of the geomagnetic field, *Ann. Geophys.* 15 (1997) 734–739.
- [68] R.T. Merrill, M.W. McElhinny, P.L. McFadden, The Magnetic Field of the Earth: Paleomagnetism, the Core, and the Deep Mantle, Academic Press, San Diego, 1996, 531 pp.
- [69] T.J. Dunai, Reply to comment on “Scaling factors for production rates of in situ produced cosmogenic nuclides: a critical reevaluation” by Darin Desilets, Marek Zreda, and Nathaniel Lifton, *Earth Planet. Sci. Lett.* 188 (2001) 289–298.
- [70] P. Rothwell, Cosmic rays in the Earth’s magnetic field, *Philos. Mag.* 3 (Series 8) (1958) 961–970.
- [71] N. Iucci, G. Villaresi, L.I. Dorman, M. Parisi, Cosmic ray survey to Antarctica and coupling functions for neutron component near solar minimum (1996–1997): 2. Determination of meteorological effects, *J. Geophys. Res.* 105 (2000) 21035–21045.
- [72] G. Bonani, G. Cini Castagnoli, C. Taricco, N. Bhandari, Heliospheric modulation of cosmic rays during prolonged solar minima deduced from cosmogenic radioisotopes in meteorites, *Adv. Space Res.* 19 (1997) 937–940.
- [73] G. Cini Castagnoli, G. Bonino, C. Taricco, S.M. Bernasconi, Solar radiation variability in the last 1400 years recorded in the carbon isotope ratio of a Mediterranean Sea core, *Adv. Space Res.* 29 (2002) 1989–1994.
- [74] M. Lockwood, Twenty-three cycles of changing open solar magnetic flux, *J. Geophys. Res.* 108 (2003) 1128, doi:10.1029/2002JA009431.

- [75] K.G. McCracken, Variations in the production of ^{10}Be due to the 11 year modulation of the cosmic radiation, and variations in the vector geomagnetic dipole, in: W. Droege, H. Kunow, M. Scholer (Eds.), 27th International Cosmic-Ray Conference Solar and Heliospheric Phenomena, Copernicus Gesellschaft, Hamburg, Germany, 2001, pp. 4129–4132.
- [76] G.M. Raisbeck, F. Yiou, J. Jouzel, J.R. Petit, ^{10}Be and $\delta^2\text{H}$ in polar ice cores as a probe of the solar variability's influence on climate, *Philos. Trans. R. Soc. Lond. Ser. A: Math. Phys. Sci.* A330 (1990) 463–470.
- [77] J. Beer, S. Baumgartner, B. Dittrich-Hannen, J. Hauenstein, P. Kubik, C. Lukaszczuk, W. Mende, R. Stellmacher, M. Suter, Solar variability traced by cosmogenic isotopes, in: J.M. Pap, C. Fröhlich, H.S. Hudson, S.K. Solanki (Eds.), *The Sun as a Variable Star: Solar and Stellar Irradiance Variations*, Cambridge University Press, 1994, pp. 291–300.
- [78] J. Beer, R. Muscheler, G. Wagner, C. Laj, C. Kissel, P.W. Kubik, H.-A. Synal, Cosmogenic nuclides during isotope stages 2 and 3, *Quat. Sci. Rev.* 21 (2002) 1129–1139.
- [79] S.K. Solanki, I.G. Usoskin, B. Kromer, M. Schüssler, J. Beer, Unusual activity of the Sun during recent decades compared to the previous 11,000 years, *Nature* 431 (2004) 1084–1087.
- [80] I.G. Usoskin, K. Mursula, S. Solanki, M. Schüssler, K. Alanko, Reconstruction of solar activity for the last millennium using ^{10}Be data, *Astron. Astrophys.* 413 (2004) 745–751.
- [81] R.A. Caballero-Lopez, H. Moraal, K.G. McCracken, F.B. McDonald, The heliospheric magnetic field from 850 to 2000 AD inferred from ^{10}Be records, *J. Geophys. Res.* 109 (2004), doi:10.1029/2004JA010633.
- [82] K.G. McCracken, F.B. McDonald, J. Beer, G. Raisbeck, F. Yiou, A phenomenological study of the long-term cosmic ray modulation, 850–1958 AD, *J. Geophys. Res.* 109 (2004), doi:10.1029/2004JA010685.
- [83] K.G. McCracken, Geomagnetic and atmospheric effects upon the cosmogenic ^{10}Be observed in polar ice, *J. Geophys. Res.* 109 (2004), doi:10.1029/2003JA010060.
- [84] I.G. Usoskin, S.K. Solanki, M. Schüssler, K. Mursula, K. Alanko, Millennium-scale sunspot number reconstruction: evidence for an unusually active sun since the 1940s, *Phys. Rev. Lett.* 91 (2003) 211101-1–211101-4.
- [85] I.G. Usoskin, B. Kromer, Reconstruction of the ^{14}C production rate from measured relative abundance, *Radiocarbon* 47 (1) (2005) 31–37.
- [86] J. Beer, A. Blinov, G. Bonani, R.C. Finkel, H.J. Hofmann, B. Lehmann, H. Oeschger, A. Sigg, J. Schwander, T. Staffellbach, B. Stauffer, M. Suter, W. Wölfli, Use of ^{10}Be in polar ice to trace the 11-year cycle of solar activity, *Nature* 347 (1990) 164–166.
- [87] E.J. Steig, P.J. Polissar, M. Stuiver, P.M. Grootes, R.C. Finkel, Large amplitude solar modulation cycles of ^{10}Be in Antarctica: implications for atmospheric mixing processes and interpretation of the ice core record, *Geophys. Res. Lett.* 23 (1996) 523–526.
- [88] E. Bard, G.M. Raisbeck, F. Yiou, J. Jouzel, Solar modulation of cosmogenic nuclide production over the last millennium: comparison between ^{14}C and ^{10}Be records, *Earth Planet. Sci. Lett.* 150 (1997) 453–462.
- [89] R.C. Reedy, J.R. Arnold, Interaction of solar and galactic cosmic-ray particles with the Moon, *J. Geophys. Res.* 77 (1972) 537–555.
- [90] C. Tuniz, C.M. Smith, R.K. Moniot, T.H. Kruse, W. Savin, D.K. Pal, G.F. Herzog, Beryllium-10 contents of core samples from the St. Severin meteorite, *Geochim. Cosmochim. Acta* 48 (1984) 1867–1872.
- [91] M.S. Gordon, P. Goldhagen, K.P. Rodbell, T.H. Zabel, H.H.K. Tang, J.M. Clem, P. Bailey, Measurement of the flux and energy spectrum of cosmic-ray induced neutrons on the ground, *IEEE Trans. Nucl. Sci.* 51 (2004) 3427–3434.
- [92] E.B. Hughes, P.L. Marsden, Response of a standard IGY neutron monitor, *J. Geophys. Res.* 71 (1966) 1435–1444.
- [93] Measurement and reporting of alpha particle and terrestrial cosmic ray-induced soft errors in semiconductor devices, JEDEC Standard JESD89, JEDEC Solid State Technology Association, 2001, pp. 1–64.
- [94] W.N. Hess, H.W. Patterson, R. Wallace, Cosmic-ray neutron energy spectrum, *Phys. Rev., Ser. A* 116 (1959) 445–457.
- [95] K. O'Brien, A.d.I.Z. Lerner, M.A. Shea, D.F. Smart, The production of cosmogenic isotopes in the Earth's atmosphere and their inventories, in: C.P. Sonett, M.S. Giampapa, M.S. Matthews (Eds.), *The Sun in Time*, The University of Arizona, Tucson, AZ, 1991, pp. 317–342.
- [96] J. Masarik, J. Beer, Simulation of particle fluxes and cosmogenic nuclide production in the Earth's atmosphere, *J. Geophys. Res.* 104 (1999) 12099–12111.
- [97] G. Castagnoli, D. Lal, Solar modulation effects in terrestrial production of carbon-14, *Radiocarbon* 22 (1980) 133–158.
- [98] I.G. Usoskin, K. Alanko, K. Mursula, G.A. Kovaltsov, Heliospheric modulation strength during the neutron monitor era, *Sol. Phys.* 207 (2002) 389–399.
- [99] M. Merker, E.S. Light, H.J. Verschell, R.B. Mendell, S.A. Korff, Time dependent worldwide distribution of atmospheric neutrons and of their products: 1. Fast neutron observations, *J. Geophys. Res.* 78 (1973) 2727–2740.
- [100] T.E. Cerling, H. Craig, Cosmogenic ^3He production rates from 39°N to 46°N latitude, western USA and France, *Geochim. Cosmochim. Acta* 58 (1994) 249–255.
- [101] D.H. Clark, P.R. Bierman, P. Larsen, Improving in situ cosmogenic chronometers, *Quat. Res.* 44 (1995) 367–377.
- [102] P.W. Kubik, S. Ivy-Ochs, J. Masarik, M. Frank, C. Schlüchter, ^{10}Be and ^{26}Al production rates deduced from an instantaneous event within the dendro-calibration curve, the landslide of Köfels, Ötz Valley, Austria, *Earth Planet. Sci. Lett.* 161 (1998) 231–241.
- [103] M.D. Kurz, In situ production of terrestrial cosmogenic helium and some applications to geochronology, *Geochim. Cosmochim. Acta* 50 (1986) 2855–2862.
- [104] N.A. Lifton, A.J.T. Jull, J. Quade, A new extraction technique and production rate estimate for in situ cosmogenic ^{14}C in quartz, *Geochim. Cosmochim. Acta* 65 (2001) 1953–1969.
- [105] K. Nishiizumi, E.L. Winterer, C.P. Kohl, J. Klein, R. Middleton, D. Lal, J.R. Arnold, Cosmic ray production rates of

- ^{10}Be and ^{26}Al in quartz from glacially polished rocks, *J. Geophys. Res.* 94 (1989) 17907–17915.
- [106] E.T. Brown, J.M. Edmond, G.M. Raisbeck, F. Yiou, M.D. Kurz, E.J. Brook, Examination of surface exposure ages of Antarctic moraines using in situ produced ^{10}Be and ^{26}Al , *Geochim. Cosmochim. Acta* 55 (1991) 2269–2283.
- [107] F.M. Phillips, M.G. Zreda, M.R. Flinsch, D. Elmore, P. Sharma, A reevaluation of cosmogenic ^{36}Cl production rates in terrestrial rocks, *Geophys. Res. Lett.* 23 (1996) 949–952.
- [108] J.O. Stone, G.L. Allan, L.K. Fifield, R.G. Cresswell, Cosmogenic chlorine-36 from calcium spallation, *Geochim. Cosmochim. Acta* 60 (1996) 679–692.
- [109] J.O.H. Stone, J.M. Evans, L.K. Fifield, G.L. Allan, R.G. Cresswell, Cosmogenic chlorine-36 production in calcite by muons, *Geochim. Cosmochim. Acta* 62 (1998) 433–454.